May 1989

The decomposition of $[Mn(CO)_5]_2(\mu\text{-}SiH_2)$

G.T. Stauf
Syracuse University

Peter A. Dowben
University of Nebraska-Lincoln, pdowben@unl.edu

K. Emrich
Institut fur Physikalische Chemie, Freie Universitat Berlin, Takustrasse, Berlin, Federal Republic of Germany

W. Hirschwald
Institut fur Physikalische Chemie, Freie Universitat Berlin, Takustrasse, Berlin, Federal Republic of Germany

N.M. Boag
Sapord University, Sapord, England

The decomposition of $[Mn(CO)_5]_2(\mu\text{-}SiH_2)$

G. T. Stauf and P. A. Dowben
Laboratory for Solid State Science and Technology, Syracuse University, Syracuse, New York 13244-1130

K. Emrich and W. Hirschwald
Institut für Physikalische Chemie, Freie Universität Berlin, Takustrasse 3, 1000 Berlin 33, Federal Republic of Germany

N. M. Boag
Department of Chemistry and Applied Chemistry, Salford University, Salford, England, M5-4WT

(Received 16 August 1988; accepted 29 August 1988)

The prospect of using chemical vapor deposition to deposit mixed metals and silicides from a single source compound is attractive but largely uninvestigated. Studies of decomposition energies of such compounds are nearly nonexistent. One such compound which has successfully been used to make a silicide coating is $[Mn(CO)_5]_2(\mu\text{-}SiH_2)$. We have used electron impact mass spectroscopy, photoionization mass spectroscopy, and photoabsorption to determine bond energies within this compound. The combination of methods allows a high degree of confidence in the resultant ionization and fragment appearance potentials. Some possible mechanisms of decomposition are discussed. A complete ionic decomposition thermodynamic cycle has been generated, and the results are used to illuminate the coating processes previously observed.

I. INTRODUCTION

Chemical vapor deposition (CVD) from organometallic compounds is a common way of creating metal and metal silicide coatings.[1] Deposition may be induced by pyrolysis, plasma processes, or by photolysis. Silicides, metal/silicon compounds in various phases and combinations, have found favor of late in the semiconductor industry when low-resistance interconnects capable of withstanding high temperatures are needed. While some commonly used organometallic source compounds such as alkyls, chlorides, and hydrides have been heavily investigated, little research has been done on more unusual sources. At the moment, when a multicomponent coating is desired, a two- or three-gas flow-metering system is used. If a molecule such as $[Mn(CO)_5]_2(\mu\text{-}SiH_2)$ which contains both the Mn and Si in a 2:1 stoichiometric ratio could be induced to decompose, however, wasteful excesses which are now used to compensate for differing reaction rates would be avoided.

Such reactions may not be as simple as they would seem on the surface, however. For example, recent work on the one-photon photolysis of gaseous $Mn_2(CO)_{10}$ has shown that there are two different decomposition pathways: separation of a CO or the cleavage of the Mn metal–metal bond.[2] Another complication is that decomposition may be a multistep process. This sequential removal of ligands[3] has been observed to be the case with the pyrolysis of $Ga(CH_3)_3$ (Ref. 4) and $In(CH_3)_3$.[5] These elimination reactions can be a considerable problem, for example, with the release of silane from metal silyl carbonyls.[6]

$$2[Mn(CO)_5(SiH_3)] \rightarrow SiH_4 + [Mn(CO)_5]_2(SiH_2)\,.$$

Alternatively, the pyrolysis process can result in more complex elimination reactions,[7] such as in the case

$$Co(CO)_4(SiR_3) \rightarrow O(SiR_3)_2 + ?\,,$$

which leads to disiloxanes when R = H,[8] methyl,[9] or ethyl.[10] Coatings formed from this reaction have a cobalt-to-silicon ratio of 5:3, while the pyrolysis of $Fe(CO)_4(SiH_3)_2$ which follows a similar mechanism resulted in films with an iron-to-silicon ratio of 1:0.9.[7]

In order to control the decomposition of such a molecule, an understanding of the energetics of decomposition and bond breaking is certainly necessary. With few exceptions[11,12] these are poorly understood. With the aim of understanding decomposition energetics we have therefore undertaken an electron impact mass spectroscopy, photoionization mass spectroscopy, and gas-phase photoabsorption investigation of $[Mn(CO)_5]_2(\mu\text{-}SiH_2)$.

We have also demonstrated the actual feasibility of silicide coating formation with this compound via pyrolysis. The use of x-ray electron spectroscopy (XES), Auger electron spectroscopy (AES), and Rutherford backscattering spectroscopy (RBS) confirmed that the material formed was Mn_2Si. Such a metal silicide thin film is difficult to form without the use of metalorganic CVD (MOCVD). The microstructures of the films were also studied via x-ray diffraction (XRD) and scanning electron microscopy (SEM).

II. EXPERIMENTAL

The $[Mn(CO)_5]_2(\mu\text{-}SiH_2)$ complex was prepared as described previously[13,14] and purified by crystallization followed by low-pressure sublimation.

The electron impact mass spectroscopy experiments were undertaken using a molecular beam of sample vapor generated in an alumina Knudsen cell. This beam was directed into the electron impact ion source of a Varian MAT single-sector magnetic field mass spectrometer, as described previously.[15,16] Calibration, data reduction, evaluation procedure, and analysis of the fine structure of the ionization efficiency curves (IEC's) were undertaken using procedures outlined elsewhere.[17,18]

 0734-2101/89/030634-06$01.00

The fragmentation of $[Mn(CO)_5]_2(\mu\text{-}SiH_2)$ was also studied inside a high-temperature photoionization system using synchrotron radiation in the photon energy region 6–24 eV.[15] The synchrotron radiation source was the electron storage ring BESSY (Berliner Elektronenspeicherring Gesellschaft fuer Synchrotronstrahlung mbH) in Berlin, Federal Republic of Germany. The ions were detected using a Balzers QMG 511 quadrupole mass spectrometer.

Photoabsorption data on the gaseous species was collected at the Tantalus Storage Ring at the University of Wisconsin Synchrotron Radiation Facility, as has been discussed elsewhere.[15]

Pyrolysis of gaseous $[Mn(CO)_5]_2(\mu\text{-}SiH_2)$ was undertaken in a glass vacuum system pumped by a three-stage oil diffusion pump, capable of reaching a base pressure of 1×10^{-5} Torr. Solid crystals were allowed to sublimate at room temperature on one side of the deposition chamber, while on the other side the line to the vacuum pump carried away excess reactants and products. The substrates were pure nickel foils (Driver Harris Company) resistively heated with an alternating current. The temperature of the foil was monitored via a Chromel-Alumel thermocouple spot-welded to the back of the foil.

Coatings were examined while still on their substrates by SEM, XES, AES, and RBS. The instruments and procedures used have all been previously described.[19]

X-ray diffraction studies were made in transmission mode. The coating was removed from the substrate and placed on cellophane tape, then exposed for up to 15 h to ensure that any crystal structure would be revealed. The x-ray source was Cu $K\alpha$ radiation (1.542-Å wavelength).

III. RESULTS

The mass spectroscopy revealed the fragmentation behavior to be expected from this molecule. Basically, it lost successive carbonyls until it was down to a Mn_2Si core. The complete electron impact mass spectra at 25 eV can be seen in Fig. 1. It can be seen in this figure that the ion signals for $(Mn_2SiH_2)(CO)_7^+$ and $(Mn_2SiH_2)(CO)_6^+$ were too small to obtain accurate appearance potentials (AP's), so AP energies for these fragments were derived from the photoionization experiments. We did not find fragments differing only by one or two hydrogens to have very different appearance potentials. Even at the highest energy setting available on the mass spectrometer (70 eV) no additional fragments were seen, although more hydrogen loss was observed. Total Mn_2Si fragment abundance at this energy, with or without H_2 attached, was 27%. The ionization potentials (IP's) and appearance potentials we found are summarized in Table I. In most cases electron impact ionization and photoionization results were averaged to find the AP's listed in the table. Good agreement between the two techniques was found, with the largest difference of 0.4 eV present only in the case of $(Mn_2SiH_2)(CO)_3^+$.

It may be noticed that slope changes are mentioned in the caption of Table I. These come from the IEC of the parent ion. The IEC is a plot of the molecular or fragment ion intensity versus the electron (or photon) impact energy employed to ionize the gaseous species. It rises linearly until impact energy becomes high enough to access a new molecular orbital, which causes an abrupt slope increase as a new ionization pathway is reached. Of course, higher energy may also cause bond breakage and a downward slope change. These slope changes, or "breaks," also occur in fragment IEC's, but are more difficult to interpret and so have been left off Table I. More detail can be found in Ref. 15.

It should be noted that while photon impact data provide very accurate IP's of the parent and first AP's of the fragment ions due to its high degree of monochromacity, it is not as useful for obtaining higher appearance potentials (slope changes) from IEC plots due to poorer signal-to-noise ratios. Fortunately, a combination of the two ionization tech-

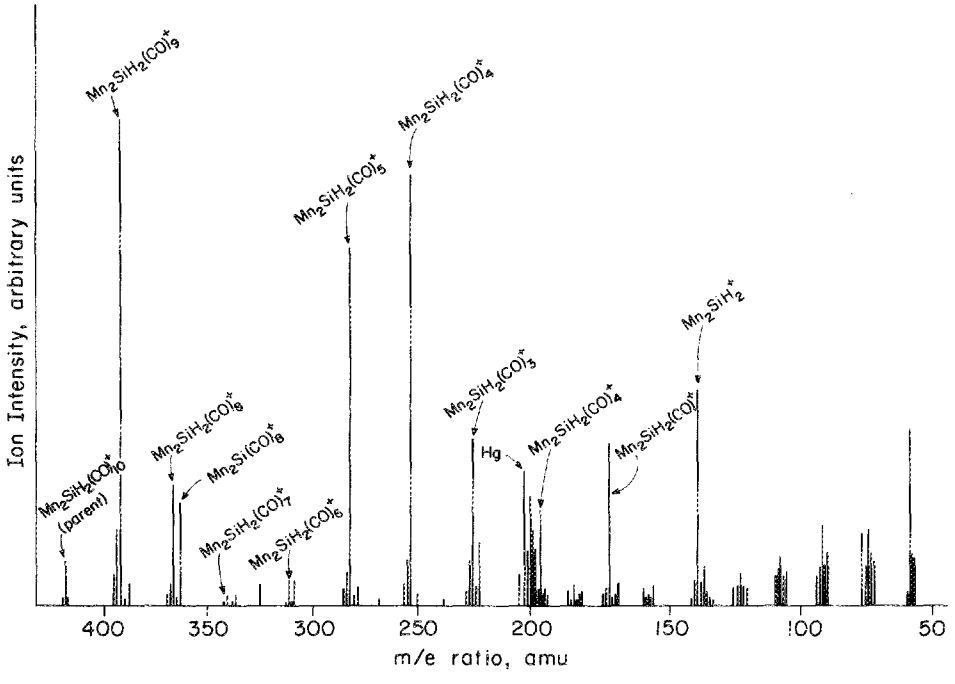

FIG. 1. Mass spectra from electron impact ionization 25-eV electron energy, for $[Mn(CO)_5]_2$ (25-eV electron energy) $(\mu\text{-}SiH_2)$.

TABLE I. The ionization and appearance potentials based on the ionization efficiency curves of $[Mn(CO)_5]_2(\mu\text{-}SiH_2)$. Arrows designate relative increases (↑) and decreases (↓) of slope in the parent IEC's. Initial AP's are given both for electron and photoionization data, which are then averaged below, while higher AP's are from electron impact data only. Values are given in eV and rounded to tenths, as estimated error is ± 0.1 eV.

Species	AP (eV)	Relative increase (↑) or decrease (↓) of slope in parent IEC	*m/e* ratio
$[Mn(CO)_5]_2(SiH_2)^+$ (parent ion)	7.9 (electron)		420
	7.9 (photo)		
	7.9 (avg.)	↑	
	8.5	↑	
	8.7	↑	
	9.0	↑	
	10.4	↓	
	12.7	↓	
	13.8	↓	
	14.8	↑	
	15.9	↑	
	17.4	↑	
$Mn_2SiH_2(CO)_9^+$	8.4 (avg.)		392
$Mn_2SiH_2(CO)_8^+$	9.4 (avg.)		364
$Mn_2SiH_2(CO)_7^+$	10.7 (photo)		336
$Mn_2SiH_2(CO)_6^+$	11.0 (photo)		308
$Mn_2SiH_2(CO)_5^+$	12.6 (avg.)		280
$Mn_2SiH_2(CO)_4^+$	13.6 (avg.)		252
$Mn_2SiH_2(CO)_3^+$	14.7 (avg.)		224
$Mn_2SiH_2(CO)_2^+$	16.4 (electron)		196
$Mn_2SiH_2(CO)_1^+$	17.1 (avg.)		168
Mn_2SiH^+	18.9 (avg.)		140

niques acts to eliminate the uncertainties associated with either one alone.

The relative intensities of the parent and fragment ions are seen plotted in Fig. 2. They are based on electron impact data, because the magnetic sector mass spectrometer used for the electron impact studies was capable of better mass resolution than the quadrupole mass spectrometer used for photoionization, and was able to easily distinguish a 2-amu separation.

The gas-phase photoabsorption curve for this compound exhibited several peaks or absorption bands. The energies at which these were observed served to confirm the AP values in Table I.[15]

Having collected thermodynamic information from various sources, we made coatings by pyrolysis of $(\mu\text{-}SiH_2)[Mn(CO)_5]_2$ as described above. Our results have been reported in the literature.[19] This particular organometallic compound has not been previously studied for purposes of coating production. Pyrolysis of our complex was found to start at ~225 °C. Coatings were black to the eye as in the case of pure metal coatings we have previously made by pyrolysis.[16]

Scanning electron microscopy showed the coatings to be smoothly granular and slightly cracked. We believe the cracks to be the result of different thermal expansion coefficients between the manganese–silicide coating and the Ni substrate, as the coatings were rather thick (over 2 μm). Despite this, the coatings showed fair adhesion.

X-ray electron spectroscopy showed by attenuation of the Ni substrate signal that the manganese silicide coatings were well over 1 μm thick after a deposition period of 1 h. This means the deposition rate was at least 170 Å/min. XES also indicated a ratio of Mn:Si of approximately 2:1, based on relative peak heights.[19]

A coating formed at high temperatures (≈550 °C) was examined by transmission x-ray diffraction, as described in the experiment section. Even with long exposure only a couple of faint, broad, evenly spaced rings became visible on the photographic film, indicating that the coating had either an amorphous microstructure or very fine microcrystallites (< 10 Å).[20]

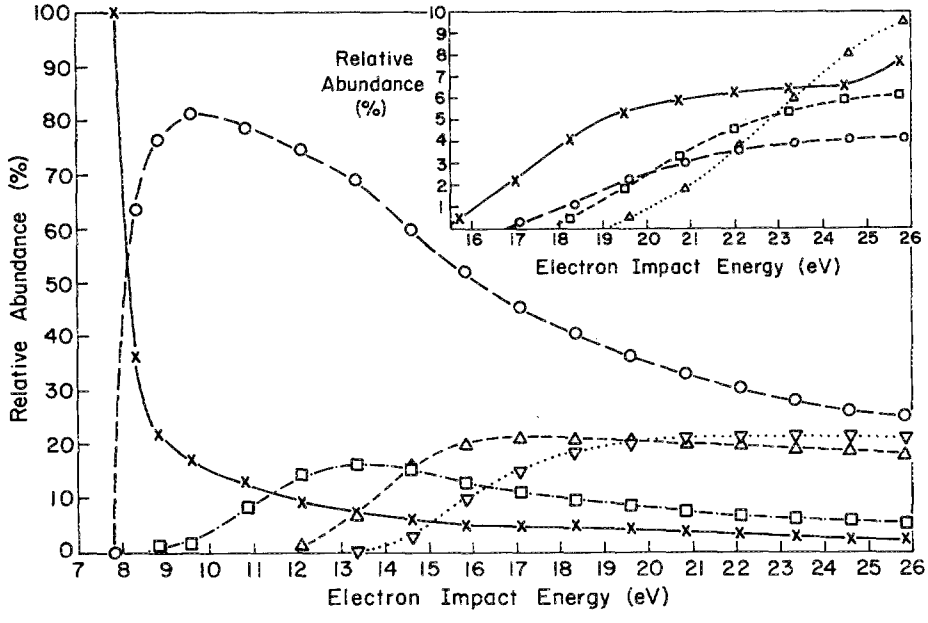

FIG. 2. The breakdown diagrams for $[Mn(CO)_5]_2(\mu\text{-}SiH_2)$ derived from electron impact IEC's. Relative intensities are plotted as a function of electron impact energy, with an intensity of 100% implying that this is the only observed fragment. Main plot: ×-parent $(Mn_2SiH_2)(CO)_{10}^+$ ion, O--$(Mn_2SiH_2)(CO)_9^+$, □···$(Mn_2SiH_2)(CO)_8^+$, △---$(Mn_2SiH_2)(CO)_5^+$, and ▽···$(Mn_2SiH_2)(CO)_4^+$. Corner inset plot: ×-$(Mn_2SiH_2)(CO)_3^+$, O-·-$(Mn_2SiH_2)(CO)_2^+$, □---$(Mn_2SiH_2)(CO)^+$, △—$(Mn_2SiH_2)^+$.

Auger electron spectroscopy was the primary method used for compositional analysis of the thin films. AES spectra were collected for coatings made at a variety of different substrate temperatures. Argon ion sputtering was used in each case to remove the top 200–300 Å of the surface in order that the underlying material composition could be assessed without surface contamination, providing of course that ion-induced mixing and preferential sputtering are negligible.[21] Auger analysis was performed at intervals during the sputtering process, thus producing a depth profile of elements. With the aid of these spectra, a plot of average bulk composition of the films versus substrate temperature at formation was created. This plot can be seen in Fig. 3.

Rutherford backscattering spectroscopy also provided very useful information on coating structure and composition. When He^+ incidence angles of 7° and 45° were used, the resulting spectra were virtually identical, indicating homogeneity throughout the bulk of the coating. Computer modeling of the spectra suggests that the thin films deposited at 500 °C are composed of a surface region, 775 Å thick, for which the composition (at. %) is 38% Mn and 19% Si, the rest being oxygen. Below this surface layer, the bulk of the sample is estimated from modeling to be 44% Mn, 22% Si, and 33% O for the films deposited at 400, 450, and 500 °C, respectively.

The Mn_2Si coating was found by RBS to be 3.4 μm thick, following a 1-h exposure of the nickel foil at 500 °C. This corresponds to a deposition rate of 570 Å/s. The films made at lower temperatures (though still above 250 °C) were thicker than this. Carbon concentration was found to be 5% or less for films deposited at 400, 450, and 500 °C, while oxygen was $<33\%$.

The manganese edge was found to become less abrupt and cornerlike at higher film deposition temperatures. This is explained by an increasing amount of oxygen (with increasing temperature from 400–500 °C) in a 2000-Å selvedge region near the surface.

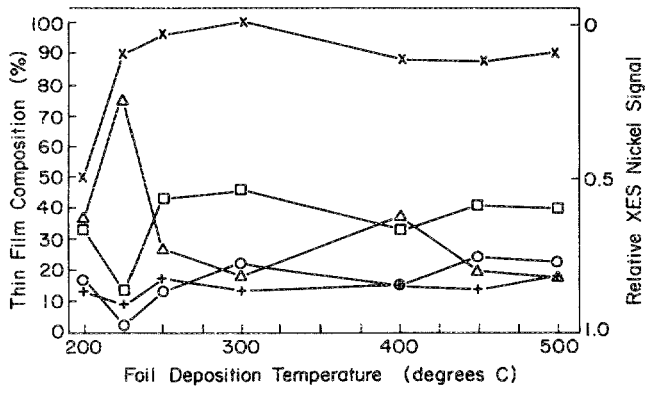

FIG. 3. The composition (AES) of films formed via the thermal decomposition of $(\mu\text{-}SiH_2)$ $[Mn(CO)_5]_2$ as a function of the foil temperature. Sputtering as mentioned previously was performed to remove surface contamination, but no correction has been made for ion mixing or preferential sputtering. The attenuation of the XES nickel signal has also been plotted (×) to provide an indication of the coating thickness. ×– inverse Ni seen (right axis), □– Mn signal seen, ○– Si signal, △– carbon signal, and + – oxygen signal.

IV. DISCUSSION

Table I shows both the higher appearance potentials of the parent IEC and the AP's of the fragment ions. An increase in the slope of the parent ion IEC is seen at 8.5 eV, close to the 8.4 eV at which the $(Mn_2SiH_2)(CO)_9^+$ ion appears. This indicates that the fragmentation mechanism involves a predissociation excitation, i.e., dissociation associated with an electronic excitation to an antibonding orbital. This partial filling of an antibonding orbital would weaken the carbonyl–metal bond leading to creation of the $(Mn_2SiH_2)(CO)_9^+$ ion. A downward slope change would indicate a direct bond breakage between the parent and the associated carbonyl fragments, since it decreases the amount of parent ion present while increasing the amount of the fragment ion seen. These conclusions have been presented in more detail previously,[15] and have been supported by our photoabsorption experiments.

From the IP and AP information in Table I, we were able to construct an ionic thermodynamic cycle for this compound.[15] This thermodynamic cycle is shown in Fig. 4. We can then conclude that the total energy to go from the parent carbonyl to the Mn_2SiH_2 core is

$$D[(Mn_2SiH_2)(CO)_{10}^+ - 10(CO)]$$
$$= AP[MN_2SiH_2^+] - IP[(Mn_2SiH_2)(CO)_{10}]$$
$$= 18.9 - 7.9 = 11.0\ \text{eV}.$$

From the relative abundances of the parent ion and different fragment ions (shown in Fig. 2) the $(Mn_2SiH_2)(CO)_{10}^+$

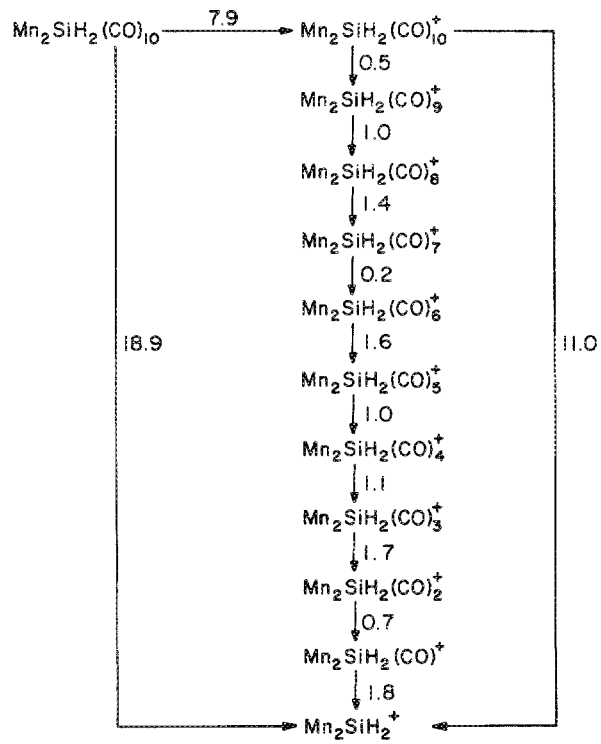

FIG. 4. The decomposition thermodynamic cycle for ionic fragmentation of $[Mn(CO)_5]_2$ $(\mu\text{-}SiH_2)$, constructed from the AP/IP information in Table I. The average AP and IP values listed (average between electron and photoionization data) were used. All numbers are in units of eV.

parent ion is seen to readily dissociate at energies greater than the appearance potential at ~8 eV. The first (and at low energies certainly the major) fragment formed is $(Mn_2SiH_2)(CO)_9^+$. Other fragments put in appearances at higher energies, and for the most part remain relatively constant in percentage composition. An exception is the $Mn_2SiH_2^+$ fragment, which increases in percentage abundance with increasing electron impact energy range near 26 eV. This indicates that even in the high electron impact energy environment of a plasma, the core manganese–silicide cluster would survive the stripping away of carbonyl ligands, offering hope of deposition as a thin film with a well-defined metal-to-silicon ratio of 2:1. The bonds between the two Mn's and the Si are obviously stronger than the bonds between each Mn and its CO ligands. The activation energy for CO cleavage from $[Mn(CO)_5]_2(\mu\text{-}SiH_2)$ is similar to that observed for other metal carbonyl species,[22–26] indicating that this molecule is fairly representative of the metal carbonyls despite having a three-atom metal center (μ-$SiMn_2$). The application of thermodynamics to thin-film deposition is obvious in this instance; with the right deposition parameters, the CO ligands will be removed while leaving the proper stoichiometric Mn:Si ratio.

Results of pyrolytic coating experiments support these statements. The primary means used to analyze composition and contaminants in these thin films were AES and RBS. Table II provides a summary of these results for coatings made at various temperatures. Discussion of the apparently rather high contamination levels follows.

From AES, the onset of thermal decomposition of $(\mu\text{-}SiH_2)\,Mn(CO)_5]_2$ on the surface of a nickel foil is at ~225 °C. At this temperature it seems that $[Mn(CO)_5]_2(SiH_2)$ is undergoing disproportionation with loss of Si, possibly in the form of silane, as discussed previously. This is leading to films with considerable carbon incorporation, and a manganese-to-silicon ratio of ≈4:1. Raising the temperature of pyrolysis eliminates this effect, however, producing the ratio 2:1 which is the same as in the source molecule. Pyrolysis of a similar compound, $Mn(CO)_5(SiH_3)$, at 773 K in a flow system, has been seen to result in a mixture of the MnSi-Mn_5Si_3 phases.[7]

The presence of carbon and oxygen in the Mn_2Si coatings at higher deposition temperatures could be the result of several different processes. One is incorporation of methane and carbon monoxide from background gases in the chamber, quite possible at a vacuum of only 10^{-5} Torr. The absence of an XRD pattern suggests that the thin film is amorphous, so impurity incorporation could occur readily without disturbing the silicide lattice structure.

Diffusion is another potential source of contamination. At high temperatures, the diffusion of carbon and oxygen from the thin film–nickel substrate interface will occur.[27] Given the cracked and granular nature of the thin film as seen in SEM photographs, we would expect a large number of interfaces akin to grain boundaries within the coating. These interfaces could provide excellent diffusion pathways for carbon and oxygen for the films prepared at 400–500 °C.

The high metal content of the thin films results in a very reactive surface, particularly with the metal manganese which oxidizes readily. The cracks and grain boundaries of the film provide additional surface area. Exposure to air, following preparation of the sample, is probably thus the origin of the heavily oxidized surface layer observed in RBS. The change in the manganese edge shape, mentioned previously, indicates that there is a gradual change in the oxygen concentration from the surface to the bulk in a selvedge region 2000 Å thick. This monotonically changing oxygen concentration is representative of oxygen diffusion from the surface after the film is deposited. If contamination were taking place during coating deposition, a uniform distribution would be expected. If it were a result of direct CO incorporation, the RBS spectra would be expected to show comparable amounts of carbon. The diffusion of oxygen into the thin film does depend on the deposition temperature at which the thin film is made. The oxygen diffusion layer was seen to have a higher concentration of oxygen near the surface with films deposited at 500 °C than at 400 °C.

As previously mentioned, Table II presents our contamination analysis. While the Auger spectroscopy did detect oxygen and carbon impurities, RBS indicated a much lower level (< 5%) of carbon than did AES (lowest number 18%). The system in which the AES was carried out was pumped with an oil diffusion pump, and it is possible that some of the carbon detected was introduced by ion mixing of surface impurities during the sputtering process. Since RBS is a less surface sensitive process, we believe it to be more representative of the true bulk composition of this coating.

TABLE II. Summary of Rutherford backscattering and Auger electron spectroscopy results for contamination and Mn:Si ratios.

Temperature (°C)	Mn-to-Si ratio		Contamination	
	AES	RBS	AES	RBS
200	1.94	· · ·	13% O, 37% C	· · ·
225	4.33	· · ·	9% O, 76% C	· · ·
250	3.30	· · ·	17% O, 27% C	· · ·
300	2.09	· · ·	13% O, 18% C	· · ·
400	2.16	2.0	15% O, 37% C	< 33% O, < 5% C
450	2.67	2.0	24% O, 20% C	< 33% O, < 5% C
500	2.10	2.0	22% O, 18% C	< 33% O, < 5% C

V. CONCLUSION

It seems then that pyrolysis of $(\mu\text{-}SiH_2)[Mn(CO)_5]_2$ does create the desired Mn_2Si compound, if the right range of substrate temperatures is maintained. The thin films that result are isotropic and uniform in content, apart from the oxygen impurities diffusing into the films from the surface. The high manganese content renders them very susceptible to oxidation upon exposure to air. If deposition and analysis were performed in UHV *in situ*, contamination levels might prove to be less than the 5% carbon and 18% oxygen indicated by our RBS and AES analyses.

The consistent 2:1 ratio of manganese to silicon from both AES and RBS at reaction temperatures over 300 °C is also very encouraging, as is the stability of the metal three-atom

center. It indicates that pyrolysis of this complex results in loss of CO, with no silyl or silane by-products created.

ACKNOWLEDGMENTS

This work was funded by the U.S. DOE through Grant No. DE-FG-02-87-ER-45319, Bundesministeriun für Forschung und Technology (BMFT) Contract No. 05313FXB3TP1, the Freie Universität Berlin, and the Syracuse University Senate. We would also like to thank the staff of the Synchrotron Radiation Center (SRC) at Stoughton, WI and BESSY (Berlin, FRG). The SRC is supported by the National Science Foundation through Grant No. DMR-86-01349.

[1]P.A. Dowben, J.T. Spencer and G.T. Stauf, Mater. Sci. Eng. B (in press).
[2]D. A. Prinslow and V. Vaida, J. Am. Chem. Soc. **109**, 5097 (1987).
[3]J. Haigh, J. Vac. Sci. Technol. B **3**, 1456 (1985).
[4]M. G. Jacko and S. J. W. Price, Can. J. Chem. **41**, 1560 (1963).
[5]M. G. Jacko and S. J. W. Price, Can. J. Chem. **42**, 1198 (1964).
[6]B. J. Aylett and J. M. Campbell, J. Chem. Soc. A **1969**, 1916.
[7]B. J. Aylett and H. M. Colquhoun, J. Chem. Soc. Dalton Trans. **1977**, 2058.
[8]B. Aylett and J. M. Campbell, J. Chem. Soc. A **1969**, 1910.
[9]Y. L. Baay and A. G. MacDiarmid, Inorg. Nucl. Chem. Lett. **3**, 159 (1967).
[10]A. J. Chalk and J. F. Harrod, J. Am. Chem. Soc. **89**, 1640 (1967).
[11]Y. J. Kime, D. C. Driscoll, and P. A. Dowben, J. Chem. Soc. Faraday Trans. 2 **83**, 403 (1987).
[12]G. T. Stauf, D. C. Driscoll, P. A. Dowben, S. Barfuss, and M. Grade, Thin Solid Films **153**, 421 (1987).
[13]B. J. Aylett and H. M. Colquhoun, J. Chem. Res. Synopses **6**, 148 (1977).
[14]K. M. Abraham and G. Urry, Inorg. Chem. **12**(12), 2850 (1973).
[15]G. T. Stauf, D. A. LaGraffe, P. A. Dowben, K. Emrich, S. Barfuss, W. Hirschwald, and N. M. Boag, Z. Naturforsch. Teil A **43**, 758 (1988).
[16]G. T. Stauf, P. A. Dowben, K. Emrich, S. Barfuss, W. Hirschwald, and N. M. Boag, J. Phys. Chem. (in press).
[17]M. Grade, J. Wienecke, W. Rosinger, and W. Hirschwald, Ber. Bunsenges. Phys. Chem. **87**, 355 (1983).
[18]W. Rosinger, M. Grade, and W. Hirschwald, Ber. Bunsenges. Phys. Chem. **87**, 536 (1983).
[19]G. T. Stauf, P. A. Dowben, N. M. Boag, L. Morales de la Garza, and S. L. Dowben, Thin Solid Films **156**, 327 (1988).
[20]D. B. Cullity, *Elements of X-Ray Diffraction*, 2nd ed. (Addison–Wesley, Reading, MA, 1978).
[21]A. W. Czanderna, "Methods and Phenomena: Their Application in Science and Technology," in *Methods of Surface Analysis*, edited by A. W. Czanderna (Elsevier, Amsterdam, 1975), Vol. 1.
[22]C. M. Melliar Smith, A. C. Adams, R. H. Kaiser, and R. A. Kushner, J. Electrochem. Soc. Solid State Sci. Technol. **121**, 298 (1974).
[23]H. E. Carlton and J. G. Oxley, AIChE J. **13**, 86 (1967).
[24]H. E. Carlton and J. G. Oxley, AIChE J. **11**, 79 (1965).
[25]R. K. Chan and R. McIntosh, Can. J. Chem. **40**, 845 (1962).
[26]J. S. Foord and R. B. Jackman, Chem. Phys. Lett. **112**, 190 (1984).
[27]P. A. Dowben and M. Grunze, J. Electron Spectrosc. Relat. Phenom. **28**, 249 (1983).